NRL Report 6207

The Effects of Unequal Radiation Loads on the Unidirectional Properties of a 36-Element Biplanar Array of Acoustic Projectors

M. A. BLIZARD

Transducer Branch
Sound Division

March 3, 1965

U.S. NAVAL RESEARCH LABORATORY
Washington, D.C.

CONTENTS

ABSTRACT

A mathematical model was derived of a 36-element, biplanar array of variable-reluctance, two-mass, quasi-dipole, acoustic projectors. It was assumed that mutual interactions and scattering may be neglected and that all projectors in the same plane have the same acoustic load. Various projector element properties and array properties were computed with the aid of an electronic digital computer as a function of frequency and several combinations of acoustic radiation loading and "arbitrary" conditions. The arbitrary conditions were (a) the separation of the two planes, (b) the phase angle by which the input voltage of the rear plane leads the input voltage of the front plane, and (c) constant and equal input current magnitudes for the two planes. The projector element properties computed were (a) the radiating surface velocity magnitude, (b) the phase angle by which the radiating surface velocity leads the input voltage, and (c) the input impedance; the array properties computed were (a) the acoustic pressure at a point in front (and in back) of the array, (b) the acoustic power, (c) the directivity index, and (d) the efficiency. The model illustrates the alteration of the unidirectional radiation of the array as a consequence of unequal radiation loads on the two planes. The model also indicates a limited improvement in the unidirectional radiation due to the addition of tuning capacitors in series with the individual projectors.

PROBLEM STATUS

This is an interim report on one phase of the problem; work is continuing.

AUTHORIZATION

NRL Problem S02-07
Project RF 001-03-44-4052

Manuscript submitted October 21, 1964.

THE EFFECTS OF UNEQUAL RADIATION LOADS ON THE UNIDIRECTIONAL PROPERTIES OF A 36-ELEMENT BIPLANAR ARRAY OF ACOUSTIC PROJECTORS

INTRODUCTION

Biplanar arrays of projector elements are characterized by the arrangement of the projectors in two planes perpendicular to a common axis (hereinafter referred to as the principal axis) and circuitry capable of maintaining different driving signals to the projector elements in the two planes. These arrays are attractive because unidirectional beam patterns exist under certain conditions without the use of pressure release materials or reflectors.

Figure 1 shows a 36-element, biplanar array of XEM-4B projector elements. The XEM-4B projector element is a variable reluctance, two-mass transducer which has a resonant frequency of about 1.8 kc. The back-to-front suppression of this array has been measured experimentally (1) for several combinations of the following "arbitrary" conditions, which are assumed to be constant with respect to frequency: The first condition is the separation d_1 of the two planes (Fig. 1). The second condition is $\arg\,(E_R/E_F)$, which is the phase angle by which E_R, the input voltage to rear plane, leads E_F, the input voltage to the front plane. The symbol arg is defined by

$$\arg\left(\frac{a + jb}{c + jd}\right) = \arctan\left(\frac{bc - ad}{ac + bd}\right) .$$

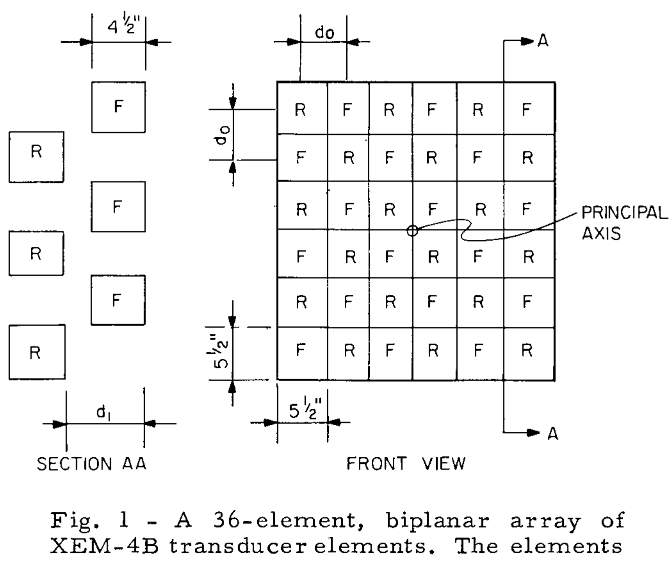

Fig. 1 - A 36-element, biplanar array of XEM-4B transducer elements. The elements denoted F and R are located in the front and rear plane respectively. The principal axis is the normal ray emerging from the center of the front view. The transducer elements vibrate in a manner such that their velocity vectors remain parallel to the principal axis.

The third condition is the equality of the magnitudes of the input currents $|I_F| = |I_R|$.

The measure of unidirectionality is back-to-front suppression $S(f)$ defined (2) by

$$S(f) = 20 \log \frac{|R(f,180°)|}{|R(f,0°)|} = 20 \log \frac{|p(f,180°)|}{|p(f,0°)|} \tag{1}$$

where $R(f,\gamma)$ is the radiation-pattern function of the array and $p(f,\gamma)$ is the acoustic pressure measured at a constant distance from the center of the array in the horizontal plane, with f being the driving frequency and γ the angular deviation of the far-field point from the principal axis.

The present report gives the derivation of a mathematical model for the 36-element, biplanar array of XEM-4B projector elements. The model is used to compute the unidirectional properties of the array for several combinations of the "arbitrary" conditions and acoustic radiation loading. Finally, the model is used to show the effect of series tuning capacitors on the unidirectional properties of the array.

DERIVATION OF THE MATHEMATICAL MODEL

The model assumes that mutual interactions and scattering may be neglected. The usefulness of this particular mathematical model of the biplanar array is diminished by the arbitrary assumptions about the acoustic radiation load seen by the transducer elements of an actual biplanar array; however, the model does illustrate the effects of unequal radiation loading on the unidirectional properties of a biplanar array.

The equations which comprise the mathematical model of the 36-element biplanar array are based on the following two "simplifying" conditions: 1. all transducers in a given plane see the same acoustic radiation load, and 2. the transducers in a given plane have the same input voltage. These two simplifying conditions and Eq. (9) imply that all projector elements in a given plane of the biplanar array have the same radiating surface velocity. It follows (3,4) that the horizontal radiation pattern function $R(f,\gamma)$ of the biplanar array is the product of the radiation pattern of the projector $H(f,\gamma)$ and two one-dimensional array pattern functions:

$$R(f,\gamma) = F(f,\gamma)\, G(f,\gamma)\, H(f,\gamma)\,. \tag{2}$$

$H(f,\gamma)$ satisfies the condition

$$H(f,\gamma) = H(f,-\gamma) = H(f,\pi-\gamma)\,.$$

The radiation pattern of either plane is given by

$$G(f,\gamma) = (1/3)\,(\cos\varphi + \cos 3\varphi + \cos 5\varphi) \tag{3}$$

where $\varphi = \pi(d_0/c)(f \sin\gamma)$ and d_0 is the intra-planar separation of elements (Fig. 1).

$F(f,\gamma)$ is a two-element endfire array pattern function given by

$$F(f,\gamma) = |u_F|\, e^{(j/2)(\psi-\psi_0)} + |u_R|\, e^{-(j/2)(\psi-\psi_0)} \tag{4}$$

where $\psi = 2\pi(d_1/c)(f \cos\gamma)$, $\psi_0 = \arg(u_R/u_F)$, and u_R and u_F are the radiating surface velocities of the projector elements in the rear and front planes respectively.

Since

$$\frac{|p(f,\pi)|}{|p(f,0)|} = \frac{|R(f,\pi)|}{|R(f,0)|} = \frac{|F(f,\pi)|}{|F(f,0)|} \tag{5}$$

the back-to-front suppression of the biplanar array is uniquely determined as soon as the plane separation d_1 and velocity distribution are specified.

For example, let $u_R/u_F = e^{j\psi_0}$. The two-element endfire array pattern function becomes

$$F(f,\gamma) = \cos (1/2)(\psi - \psi_0) \tag{6}$$

and the back-to-front suppression is given by

$$S(f) = 10 \log \frac{\left|\cos\left\{(1/2)\left[\left(2\pi \frac{d_1}{c} f\right) + \psi_0\right]\right\}\right|^2}{\left|\cos\left\{(1/2)\left[\left(2\pi \frac{d_1}{c} f\right) - \psi_0\right]\right\}\right|^2} . \tag{7}$$

The back-to-front suppression for a biplanar array satisfying the conditions $u_R/u_F = e^{j\pi/2}$ and $d_1 = 8$ in. is given in Fig. 2.

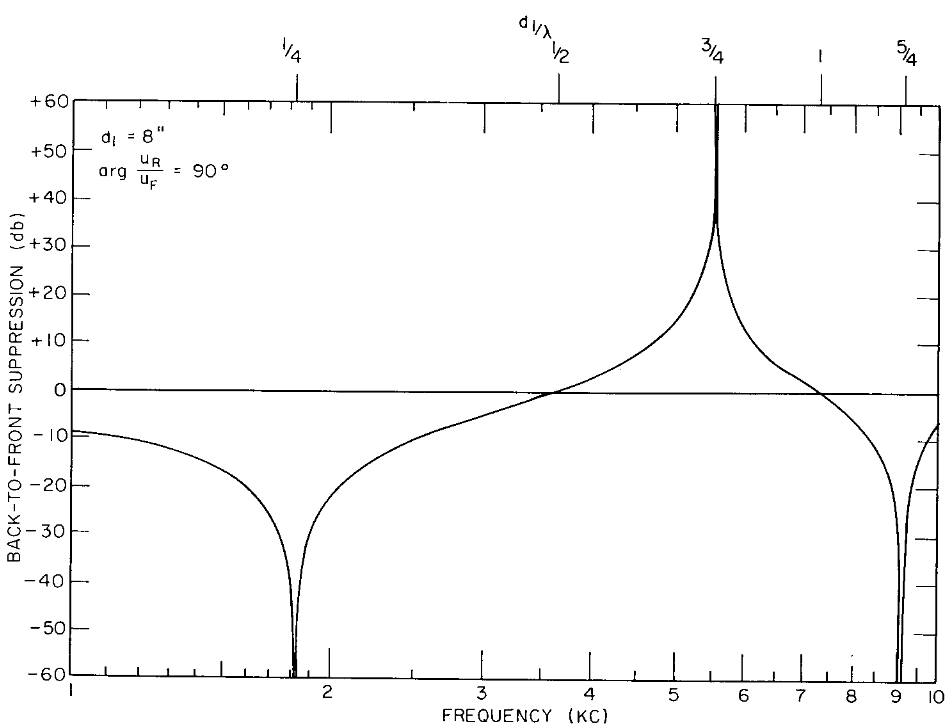

Fig. 2 - Back-to-front suppression $S(f)$ of the 36-element biplanar array for the conditions $d_1 = 8$ in. and $u_R/u_F = e^{j\pi/2}$. At $d_1/\lambda = 3/4$ the direction of the unidirectionality reverses, that is, $p(f,0) = 0$ and $p(f,\pi) \neq 0$, whereas at $d_1/\lambda = 1/4$ and $5/4$, $p(f,\pi) = 0$ and $p(f,0) \neq 0$.

The velocity distribution of a biplanar array satisfying the simplifying conditions is given by

$$\psi_0 = \arg \frac{u_R}{u_F} = \arg \frac{u_R}{E_R} + \arg \frac{E_R}{E_F} - \arg \frac{u_F}{E_F}$$

$$|u_R| = \frac{|u_R|}{|E_R|} |Z_R| \; |I_R| \qquad (8)$$

$$|u_F| = \frac{|u_F|}{|E_F|} |Z_F| \; |I_F|$$

where $|I_F| = |I_R|$ = constant and $\arg (E_R/E_F)$ = constant are "arbitrary" conditions.

The input impedances (Z_F and Z_R) as well as the quantities u_F/E_F and u_R/E_R, are functions of the parameters of the XEM-4B transducer and the radiation load on the front and rear planes of the biplanar array. These parameters are illustrated by Fig. 3.

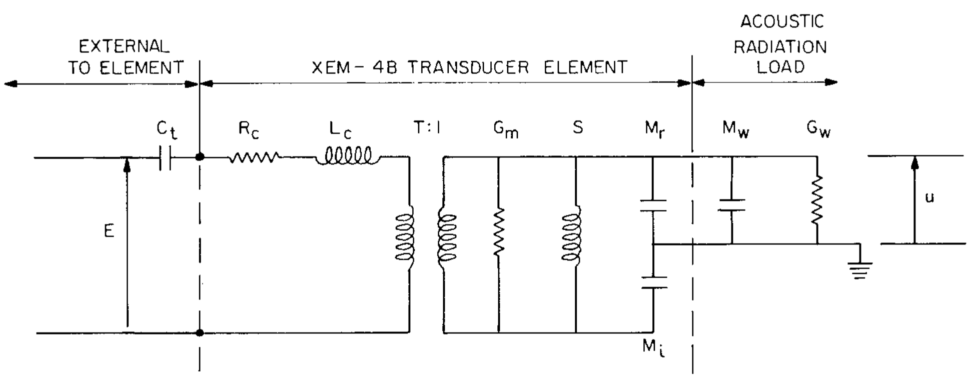

Fig. 3 - Equivalent circuit of the XEM-4B transducer, which is a two-mass, variable reluctance, single-air-gap shakerbox. From left to right, C_t is the series tuning capacitor, R_c is the clamped resistance of the element, L_c is the clamped inductance of the element, T is the turns ratio of the electromechanical transformer, G_m is the mechanical conductance of the transducer springs, S is the stiffness of the transducer springs, M_r is the outside or radiating mass, M_i is the inside or nonradiating mass, $M_w = \beta\rho cA/\omega$ is the imaginary part of the acoustic radiation load, and $G_w = \alpha\rho cA$ is the real part of the acoustic radiation load.

The velocity u of the radiating mass and the input voltage E of an XEM-4B transducer are related by the expression

$$\frac{u}{E} = \frac{j\omega M_i T}{Z(M + jN)} \qquad (9)$$

where $j = \sqrt{-1}$, $\omega = 2\pi f$ (the angular frequency),

$$M = G_m G_w + S(M_r + M_i + M_w) - \omega^2 (M_r + M_w) M_i \qquad (10)$$

and

$$N = G_m \omega (M_r + M_i + M_w) + G_w \left(\omega M_i - \frac{S}{\omega}\right). \tag{11}$$

Equation (9) and the expressions for the input impedance are based on the equivalent circuit of the XEM-4B transducer given in Fig. 3. The input impedance of the transducer element is given by

$$Z = \left(R_c + \frac{T^2 G}{G^2 + B^2}\right) + j\left(\omega L_c - \frac{T^2 B}{G^2 + B^2}\right) - \frac{j}{\omega C_t} \tag{12}$$

where

$$G = G_m + G_e \tag{13}$$

$$B = \omega M_e - \frac{S}{\omega} \tag{14}$$

in which

$$G_e = \frac{\omega^2 M_i^2 G_w}{G_w^2 + \omega^2 (M_r + M_i + M_w)^2} \tag{15}$$

$$M_e = \frac{M_i \left[G_w^2 + \omega^2 (M_r + M_w)(M_r + M_i + M_w)\right]}{G_w^2 + \omega^2 (M_r + M_i + M_w)^2}. \tag{16}$$

The clamped impedance of the projector element is

$$Z_c = R_c + j\omega L_c$$

and the impedance of the capacitor which is in series with the individual projector elements is

$$Z_{C_t} = -\frac{j}{\omega C_t}$$

where $C_t = \infty$ unless other values are stated explicitly.

The computed phase difference between u and E (i.e., $\arg(u/E)$) is plotted in Fig. 4 for several acoustic radiation loads on the XEM-4B transducer.

Equation (1), which gives the back-to-front suppression of an array, can be written as

$$S(f) = 10 \log |p(f,\pi)|^2 - 10 \log |p(f,0)|^2. \tag{17}$$

Since $|I_R| = |I_F|$ = constant (an arbitrary condition), the back-to-front suppression is the difference of two constant-current transmitting response curves (which will be plotted in decibels above 1 μbar per amp per plane at 1 meter).

The acoustic pressure produced by the biplanar array at the far-field point on the ($\gamma = 0$) portion of the principal axis is given (5) by

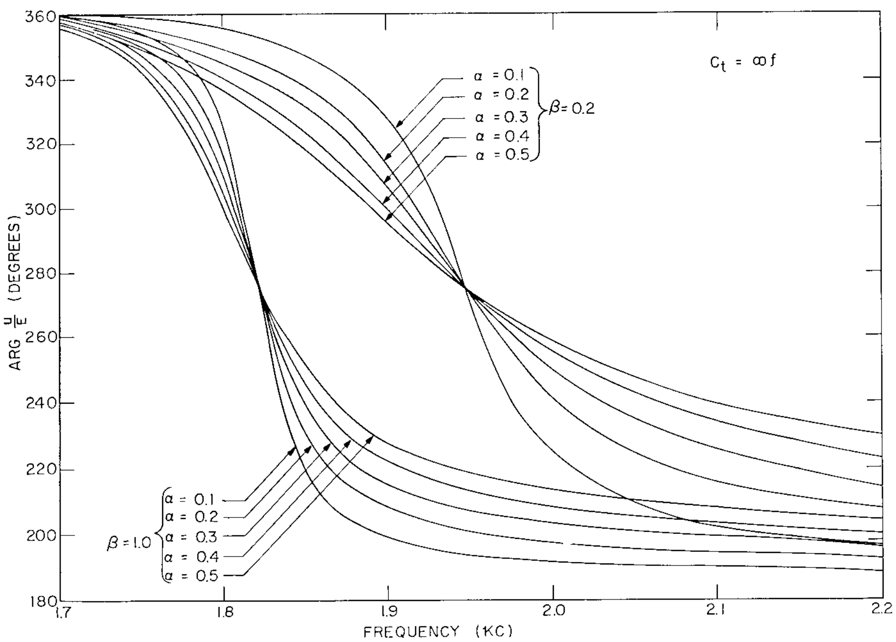

Fig. 4 - Computed phase angle (arg (u/E)) by which the radiating surface velocity of an XEM-4B transducer leads its input voltage for several acoustic radiation loads. (The symbols α and β are defined in Fig. 3.)

$$p^2(f,0) = \frac{\rho c}{4\pi r^2} \frac{P(f)}{D(f)} \tag{18}$$

where r is the distance between the array and the far-field point, ρc is the specific acoustic impedance of water, $P(f)$ is the total acoustic power generated by the array at the frequency f, and $D(f)$ is the directivity ratio of the biplanar array at the frequency f.

The acoustic power generated by the biplanar array is given by

$$P(f) = n \frac{\rho c A}{2} \left(\alpha_F \, |u_F|^2 + \alpha_R \, |u_R|^2 \right) \tag{19}$$

where $n = 18$ is the number of elements in each plane and A is the area of the radiating surface of the individual transducer element.

The directivity ratio is given approximately by

$$D(f) = \frac{1}{2} \int_0^{\pi/2} \frac{|R(f,\gamma)|^2}{|R(f,0)|^2} \sin \gamma \, d\gamma . \tag{20}$$

since the beam pattern is not an exact body of revolution.

The acoustic pressure for the field point on the $\gamma = \pi$ portion of the principal axis is given by

$$|p(f,\pi)|^2 = |p(f,0)|^2 \frac{|F(f,\pi)|^2}{|F(f,0)|^2} . \tag{21}$$

This completes the derivation of the mathematical model. The remainder of this report is devoted to the presentation of the computed properties of the array. The comparable experimental data is given where available.

NUMERICAL RESULTS

Figure 5 gives the experimental constant-current transmitting response curves for the arbitrary conditions d_1 = 8 in., $\arg(E_R/E_F)$ = 70, 90, and 110 degrees, and $|I_R| = |I_F|$ = 1 ampere.

Figure 6 gives the constant-current transmitting response curves calculated from the mathematical model for the arbitrary conditions d_1 = 8 in., $\arg(E_R/E_F)$ = 90 degrees, and $|I_R| = |I_F|$ = 1 ampere and the acoustic radiation load on the projector elements in the rear and front planes

$$Z_{a_R} = Z_{a_F}$$

where the acoustic radiation load on the projector elements is given by $Z_a = G_w + j\omega M_w = (\alpha + j\beta)\rho c A$ (see Fig. 3).

Theoretical beam patterns for the biplanar array satisfying the above conditions are given in Fig. 7 for the frequencies 1600, 1820, 1900, and 5500 cps. The frequencies 1820 and 5500 cps correspond to quarter and three-quarter wavelength spacing of the two planes of the array.

It follows from Eq. (8) and Eq. (9) that if $Z_{a_R} = Z_{a_F}$, then $u_R/u_F = e^{i\psi_0}$, where $\psi_0 = \arg(E_R/E_F)$. In this case the back-to-front suppression in Fig. 6 is the same as the back-to-front suppression in Fig. 2.

The transmitting response curves in Fig. 8 were chosen to illustrate how the back-to-front suppression is affected by changing the resistive parts of the acoustic radiation load on the array. The reactive portion of the acoustic radiation load and the arbitrary conditions are kept constant.

In Fig. 9 (along with Fig. 13(a)) the reactive part of the acoustic radiation load is varied while the arbitrary conditions and the resistive part of the acoustic radiation load are kept constant. In Fig. 9(a) the acoustic radiation loads on the two planes are almost equal. As a result the back-to-front suppression is near maximum when the two planes are $\lambda/4$ apart. In contrast, there is no back-to-front suppression at resonance in Fig. 13(a).

The parameter $\arg(E_R/E_F)$ is varied in Fig. 10, while the plane spacing d_1 and the acoustic radiation load are held constant. This particular illustration has assumed large values for the radiation load experienced by the elements. The addition of an acoustic cavity on the transducing element is a potential approach to these assumptions, but a cavity approach is much more complicated than the above assumption in that the apparent cavity transformation of radiation load is frequency dependent.

The pair of experimental constant-current transmitting response curves given in Fig. 11(a) (arbitrary conditions d_1 = 4 in., $\arg(E_R/E_F)$ = 70 degrees, and $|I_R| = |I_F|$ = 1.0 ampere) is a typical example of the experimental transmitting response curves for the biplanar array satisfying $d_1 \leq$ 4-1/2 in. Figure 11(b) plots the constant-current transmitting response curves for the equal acoustic radiation load

$$Z_{a_R} = Z_{a_F} = (0.4 + j0.2)\rho c A .$$

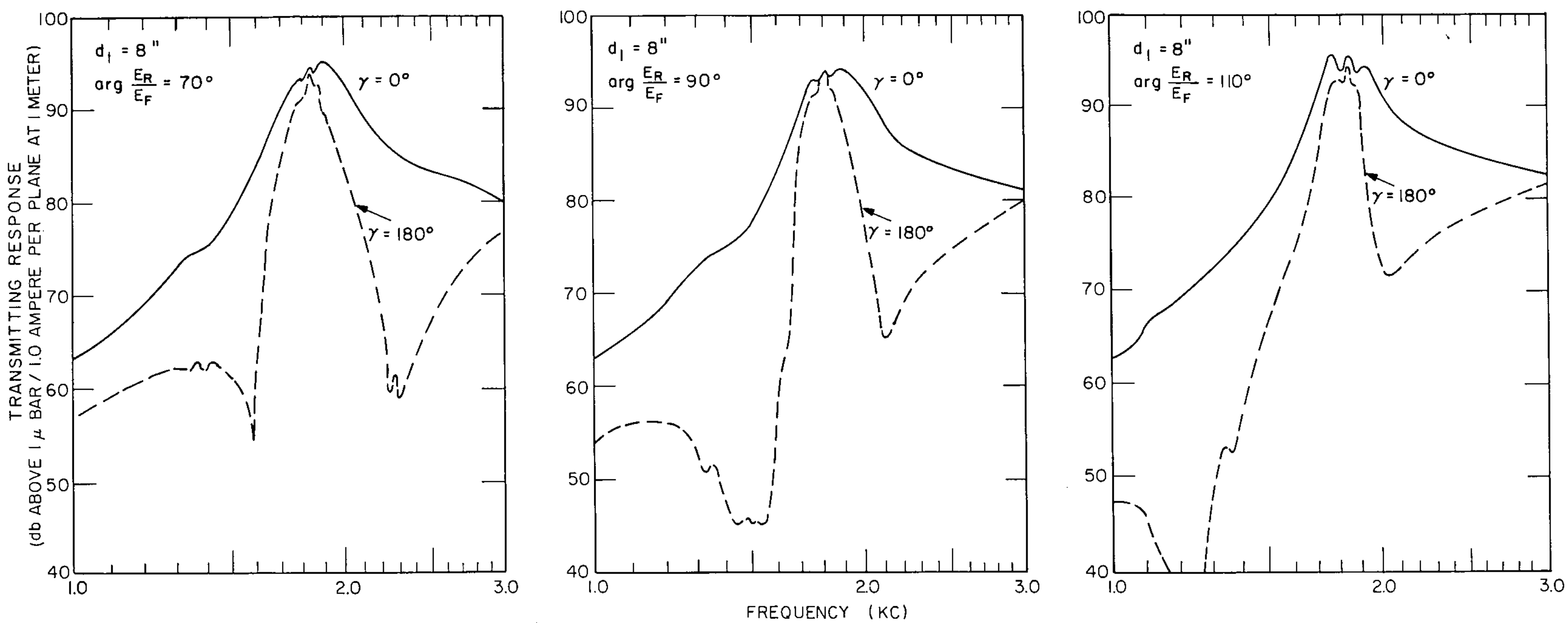

Fig. 5 - Experimental constant-current transmitting response curves for the arbitrary conditions d_1 = 8 in. and arg (E_R/E_F) = 70, 90, and 110 degrees. The $\gamma = 0^\circ$ curves show the transmitting response on the front side of the array (the constructive interference side for the two planes), and the $\gamma = 180^\circ$ curves show the transmitting response on the back side (destructive interference side).

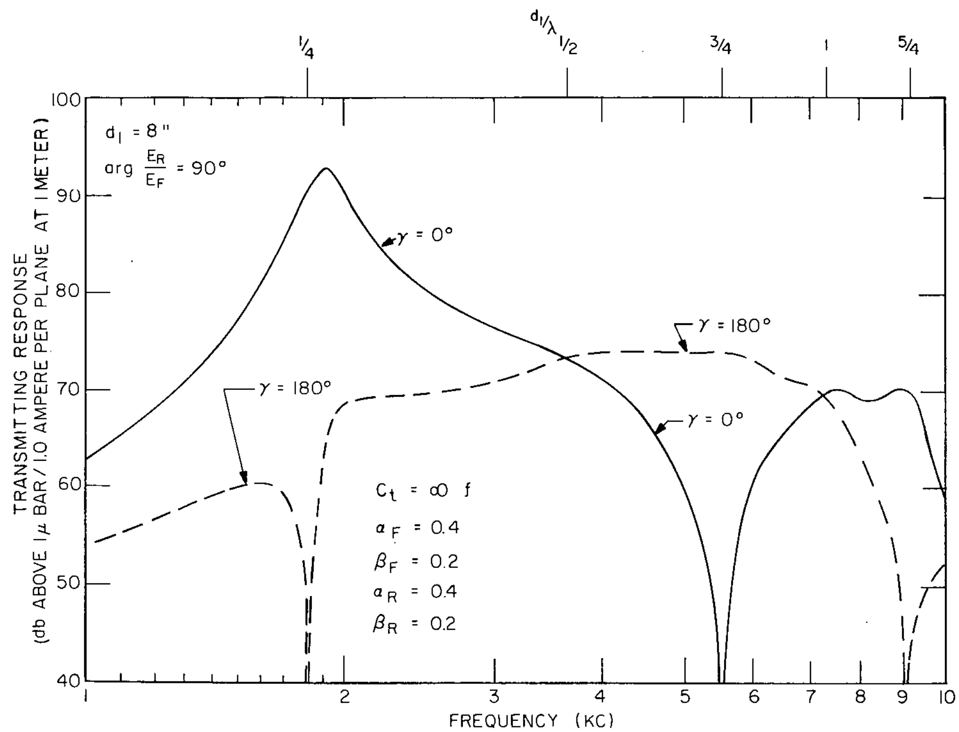

Fig. 6 - Computed constant-current transmitting response curves for the arbitrary conditions d_1 = 8 in., arg (E_R/E_F) = 90 degrees, and $|I_R| = |I_F| = 1$ ampere and the radiation load $Z_{a_R} = Z_{a_F} = (0.4 + j0.2)\rho c A$. These curves represent ideal behavior of the array for the arbitrary conditions specified.

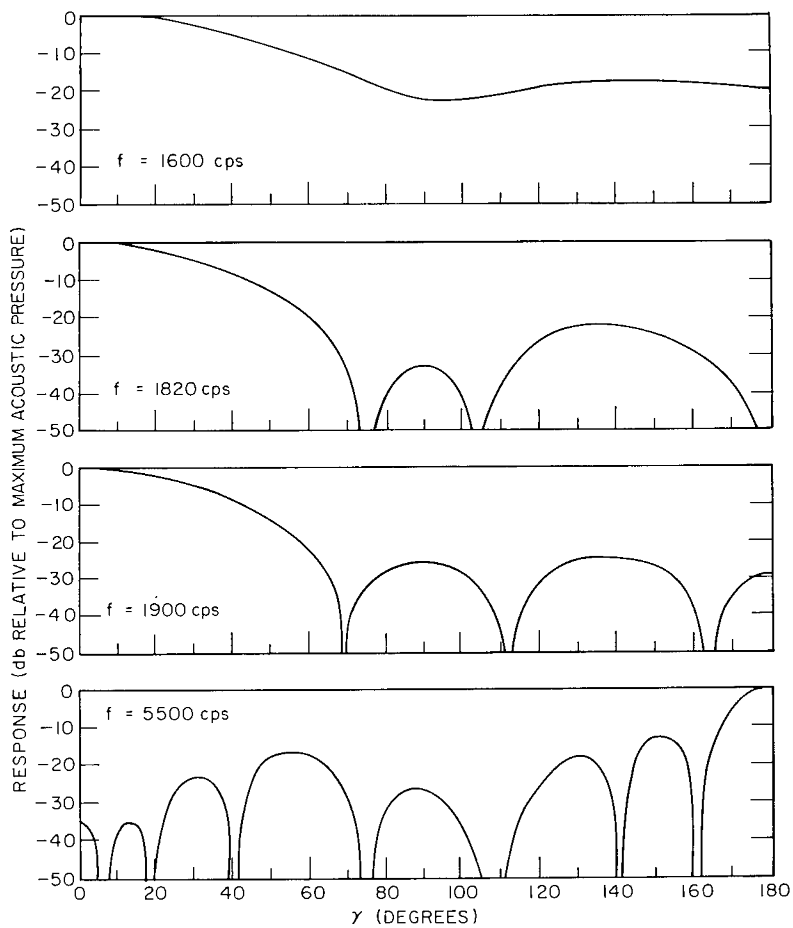

Fig. 7 - Computed beam patterns for the arbitrary conditions d_1 = 8 in., arg (E_R/E_F) = 90 degrees, and $|I_R| = |I_F| = 1$ ampere and the radiation load $z_{a_R} = z_{a_F} = (0.4 + j0.2)\rho c A$

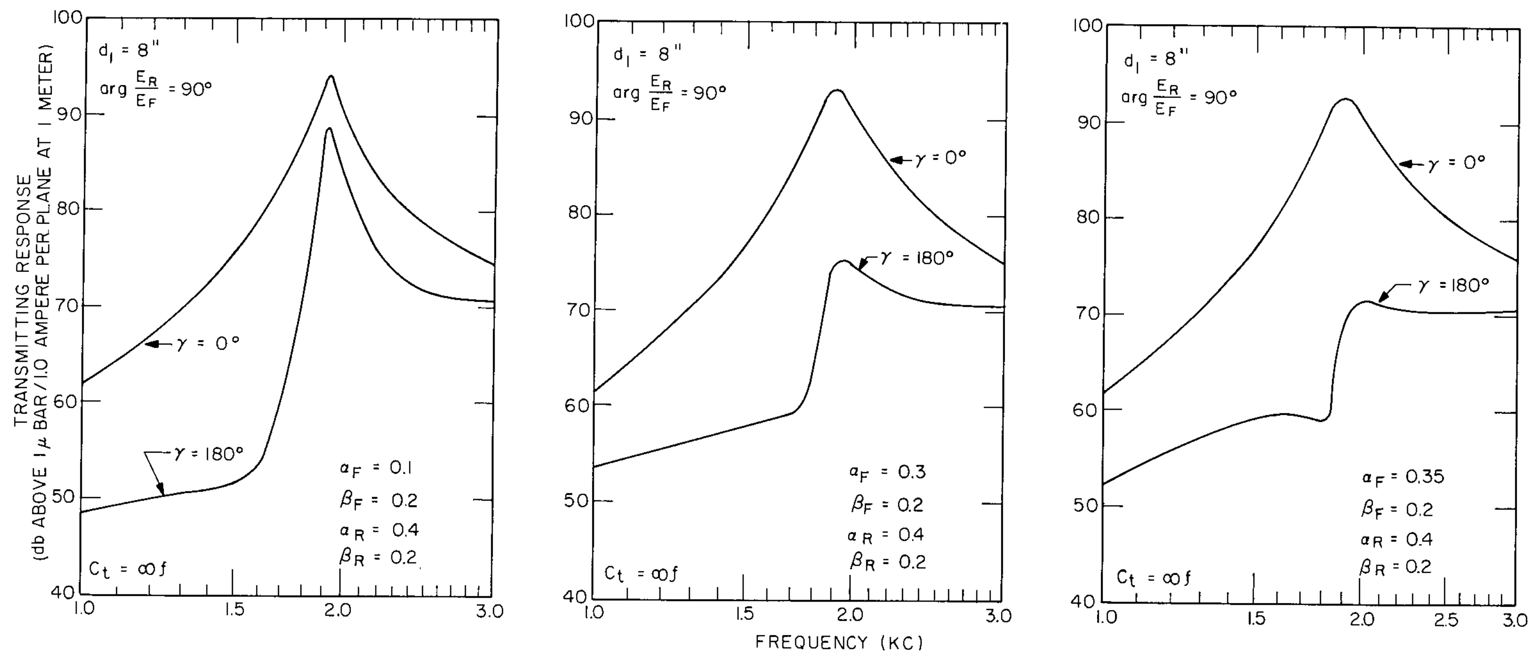

Fig. 8 - Computed constant-current transmitting response curves. The real part of the acoustic radiation load is varied, while all other parameters are held fixed. Figure 6 is a continuation of these curves, presenting the curves for α_F = 0.4.

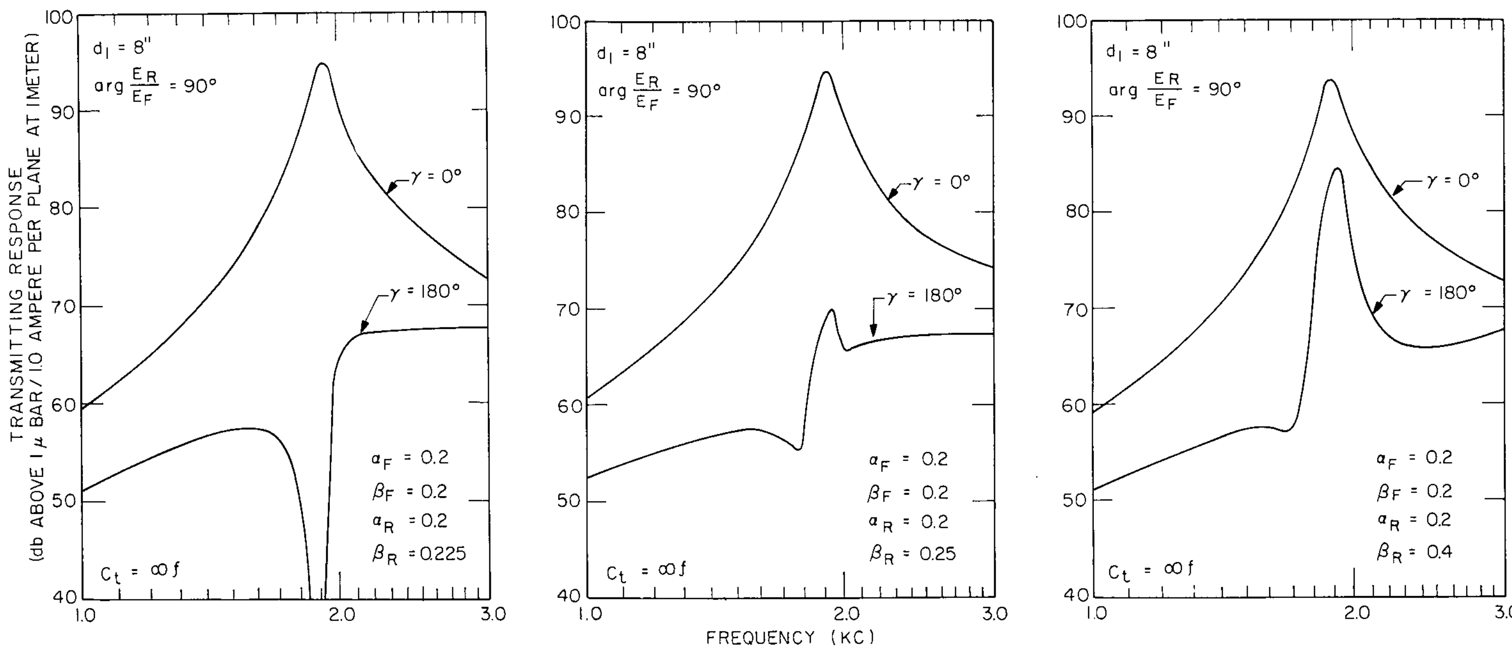

Fig. 9 - Computed constant-current transmitting response curves. The reactive part of the acoustic radiation load is varied. Figure 13(a) is a continuation of these curves, presenting the curves for $\beta_R = 0.8$.

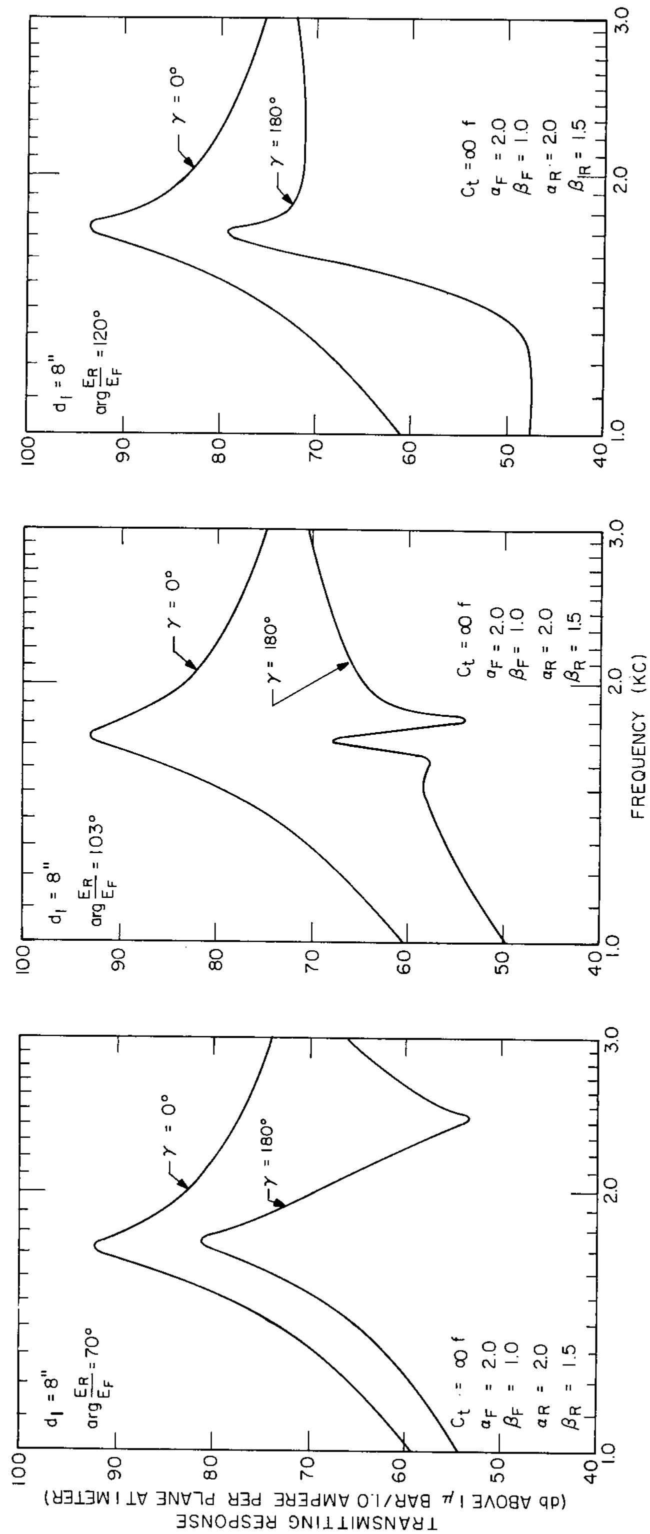

Fig. 10 - Computed constant-current transmitting response curves. The parameter arg (E_R/E_F) is varied, while d_1 and the acoustic radiation load is kept constant.

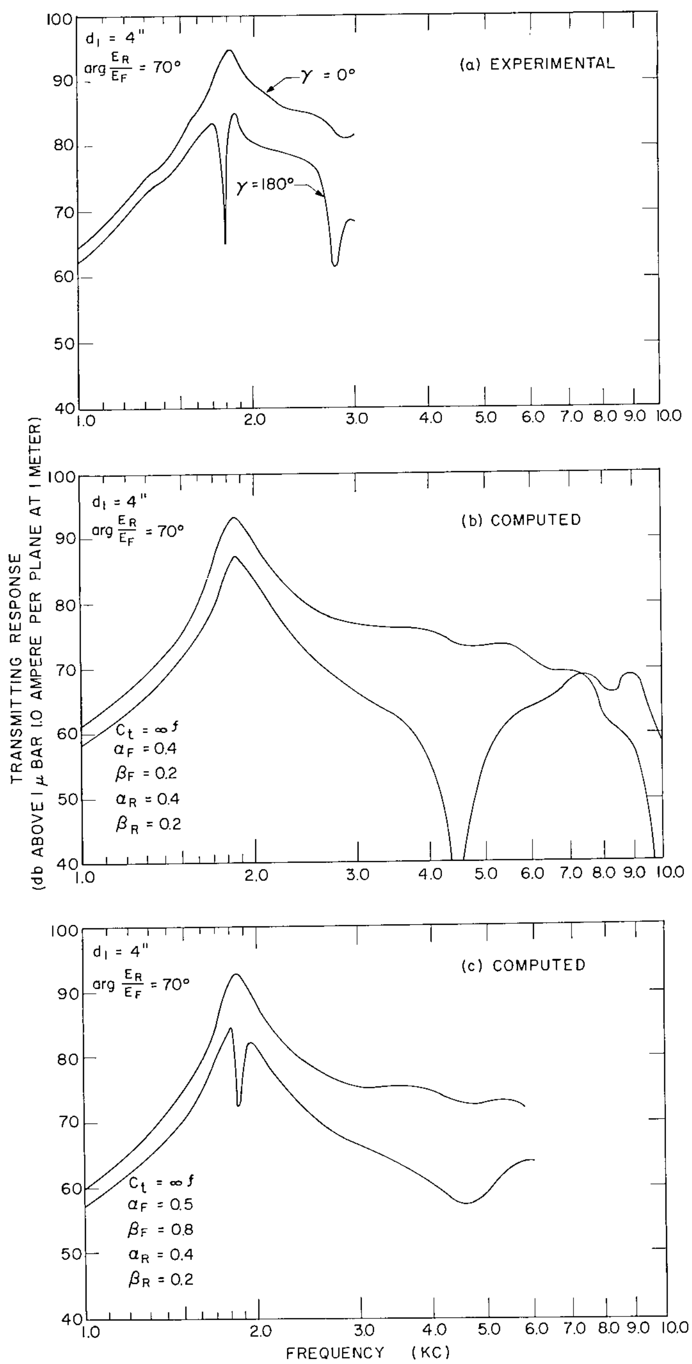

Fig. 11 - Experimental and computed constant-current transmitting response curves

Figure 11(c) gives the computed constant current transmitting response curves for the acoustic radiation load

$$Z_{a_R} = (0.4 + j0.2)\,\rho c A$$

$$Z_{a_F} = (0.5 + j0.8)\,\rho c A\,.$$

The velocity distribution on the array is given in Fig. 12.

The effect of tuning capacitors (placed in series with the individual projectors) on the back-to-front suppression of the biplanar array is demonstrated by an example. Let the array satisfy the arbitrary conditions $d_1 = 8$ in. and $\arg(E_R/E_F) = 90$ degrees and the radiation load

$$Z_{a_R} = (0.2 + j0.8)\,\rho c A$$

$$Z_{a_F} = (0.2 + j0.2)\,\rho c A$$

for the three following values of tuning capacitors: $C = \infty$ (no tuning), $C = 3.0\,\mu f$ (L_c tuned out at $f = 1.8$ kc), and $C = 1/(\omega^2 L_c)$ (L_c tuned out at all frequencies).

The constant-current transmitting response curves for these three values of capacitance are given by Fig. 13(a), Fig. 13(b), and Fig. 13(c). The back-to-front suppression at the resonant frequency (1.8 kc) is:

for $C = \infty$, $S(f) = 0$ db (Fig. 13(a)),

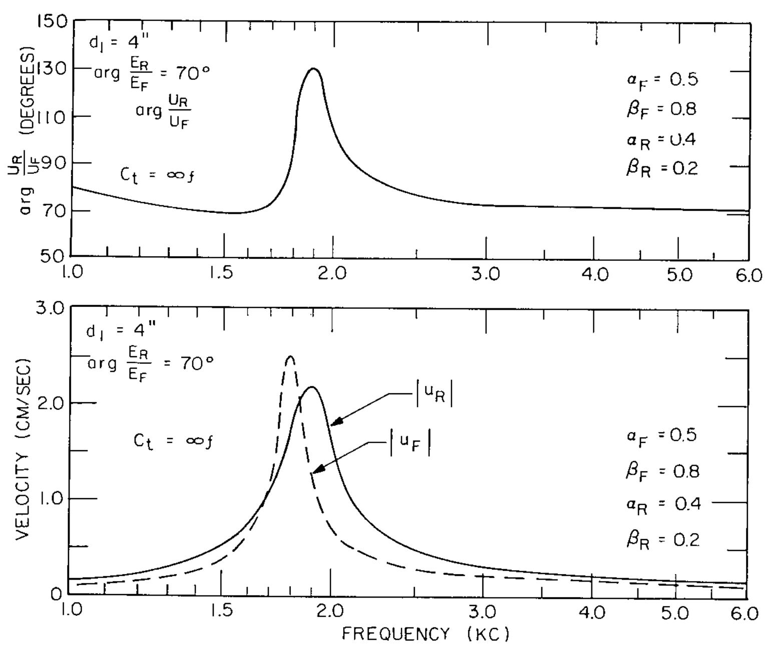

Fig. 12 - Computed velocity distribution for the acoustic radiation load and arbitrary conditions shown in Fig. 11(c)

$$\text{for } C = 3.0\,\mu f,\ S(f) = -14 \text{ db (Fig. 13(b))},$$

$$\text{for } C = \frac{1}{\omega^2 L_c},\ S(f) = -13.5 \text{ db (Fig. 13(c))}.$$

Figures 13(d), (e), and (f) are included to illustrate the importance of

$$|u_R| = |u_F| .$$

In these cases $\arg (u_R/u_F)$ is not changed and is given by Fig. 14(a).

The back-to-front suppression becomes at resonance:

$$\text{for } C = \infty,\ S(f) = 0 \text{ db},$$

$$\text{for } C = 3.0\,\mu f,\ S(f) = -17.5 \text{ db},$$

$$\text{for } C = \frac{1}{\omega^2 L_c},\ S(f) = -15.5 \text{ db}.$$

Further improvement in the back-to-front suppression can be realized by adjusting

$$\arg \frac{E_R}{E_F}$$

so that

$$\arg \frac{u_R}{u_F} = 90 \text{ degrees}$$

at $f = 1.8$ kc.

CONCLUDING REMARKS

In summary, a mathematical model of a 36-element biplanar array of XEM-4B elements has been derived. It has been used to illustrate the alteration of the unidirectional properties of the array by unequal radiation loads on the two planes as compared to the simple theory which ignores the presence of a resonant transducing element and variable radiation loading. The model indicates a limited improvement in the unidirectional properties of the array due to the addition of series tuning capacitors. The model further indicates that large, "apparent" radiation loads might produce marked improvement.

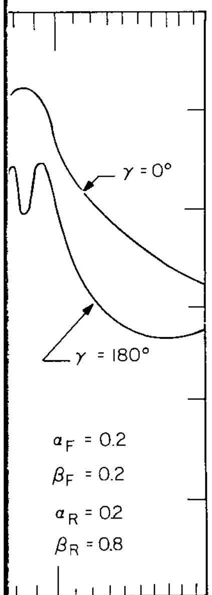

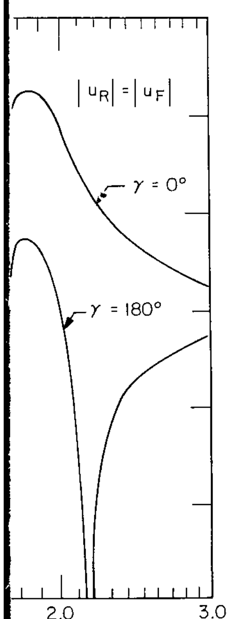

the acoustic
o $|u_R|$.

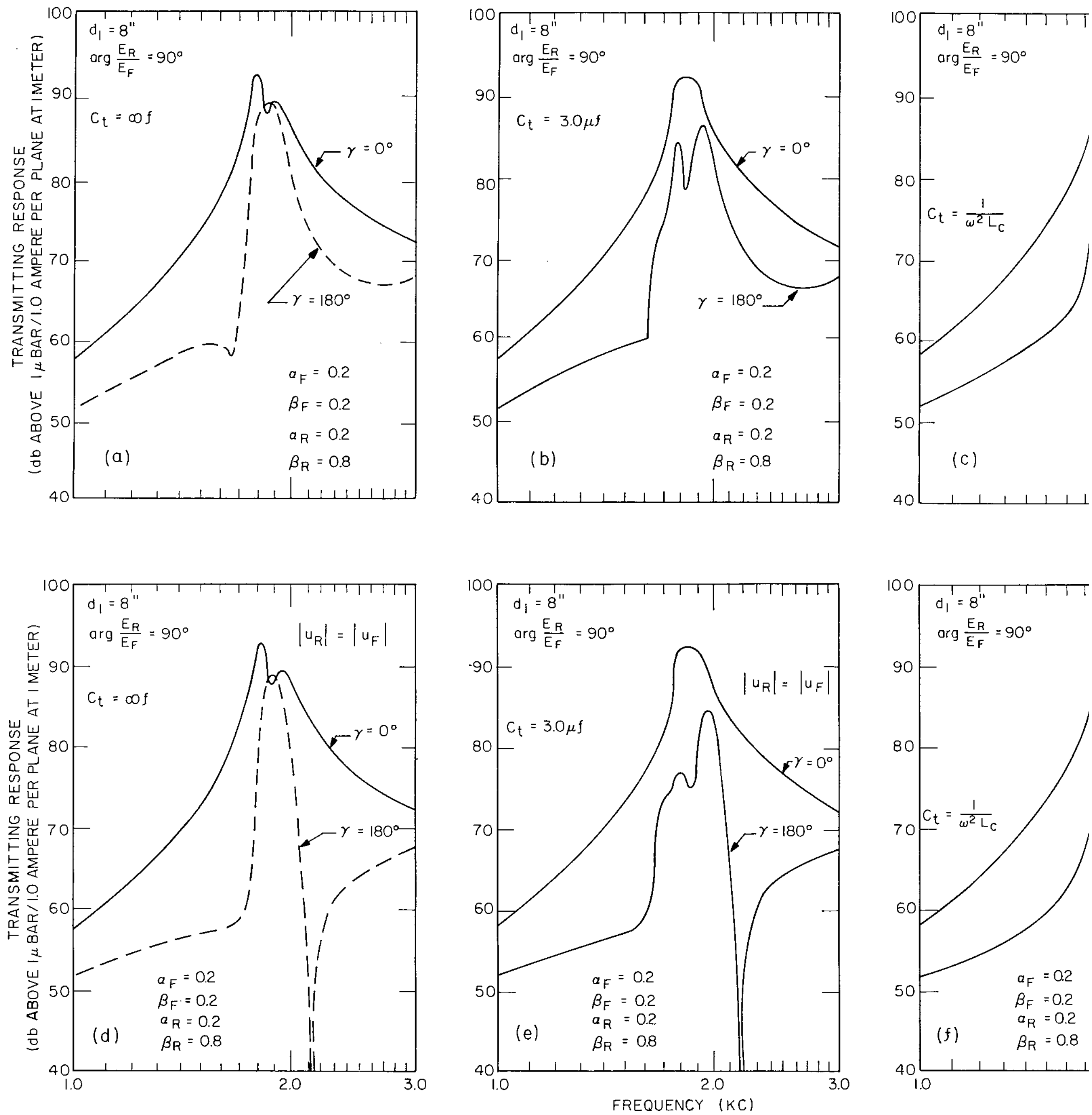

Fig. 13 - Computed constant-current transmitting response curves for the arbitrary conditions, radiation load, and the values of C_t shown. In d, e, and f, $|u_F|$ is constrained to be equal t

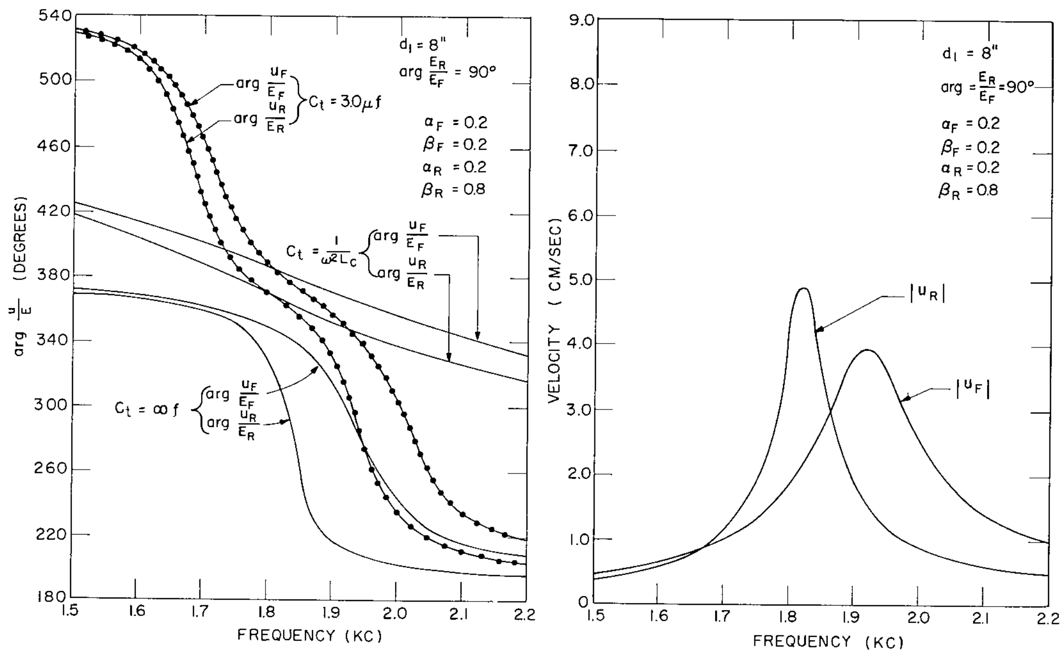

Fig. 14 - Computed velocity distribution for the values shown for the radiation load, arbitrary conditions, and three values of capacitance in series with the individual elements

REFERENCES

1. Chervenak, J., U.S. Navy J. Underwater Acoust. 11:453-462 (1961)

2. Faires, R.E., U.S. Navy J. Underwater Acoust. 11:439-451 (1961)

3. Blizard, M.A., "Optimization of the Back-to-Front Suppression and Frequency Bandwidth Relationship for Three-Dimensional Acoustic Arrays," NRL Report 6204, Feb. 12, 1965

4. Stenzel, H., "Leitfaden zur Berechnung von Schallvorgängen," Berlin:Springer, 1939

5. "The Design and Construction of Magnetostriction Transducers," Vol. 13, Summary Tech. Report of Div. 6, National Defense Research Committee, 1946

* * *

Security Classification

DOCUMENT CONTROL DATA - R&D

(Security classification of title, body of abstract and indexing annotation must be entered when the overall report is classified)

1. ORIGINATING ACTIVITY *(Corporate author)* U.S. Naval Research Laboratory Washington, D.C. 20390	2a. REPORT SECURITY CLASSIFICATION Unclassified 2b. GROUP

3. REPORT TITLE

The Effects of Unequal Radiation Loads on the Unidirectional Properties of a 36-Element Biplanar Array of Acoustic Projectors

4. DESCRIPTIVE NOTES *(Type of report and inclusive dates)*

An interim report on one phase of the problem.

5. AUTHOR(S) *(Last name, first name, initial)*

Blizard, M.A.

6. REPORT DATE March 3, 1965	7a. TOTAL NO. OF PAGES 24	7b. NO. OF REFS 5

8a. CONTRACT OR GRANT NO. NRL Problem S02-07 b. PROJECT NO. RF 001-03-44-4052 c. d.	9a. ORIGINATOR'S REPORT NUMBER(S) NRL Report 6207 9b. OTHER REPORT NO(S) *(Any other numbers that may be assigned this report)*

10. AVAILABILITY/LIMITATION NOTICES Unlimited availability. Copies available from Clearinghouse for Federal Scientific and Technical Information (CFSTI) Sills Building, 5285 Port Royal Road, Springfield, Virginia 22151.

11. SUPPLEMENTARY NOTES	12. SPONSORING MILITARY ACTIVITY Department of the Navy (Office of Naval Research)

13. ABSTRACT

A mathematical model was derived of a 36-element, biplanar array of variable-reluctance, two-mass, quasi-dipole, acoustic projectors. It was assumed that mutual interactions and scattering may be neglected and that all projectors in the same plane have the same acoustic load. Various projector element properties and array properties were computed with the aid of an electronic digital computer as a function of frequency and several combinations of acoustic radiation loading and "arbitrary" conditions. The arbitrary conditions were (a) the separation of the two planes, (b) the phase angle by which the input voltage of the rear plane leads the input voltage of the front plane, and (c) constant and equal input current magnitudes for the two planes. The projector element properties computed were (a) the radiating surface velocity magnitude, (b) the phase angle by which the radiating surface velocity leads the input voltage, and (c) the input impedance; the array properties computed were (a) the acoustic pressure at a point in front (and in back) of the array, (b) the acoustic power, (c) the directivity index, and (d) the efficiency. The model illustrates the alteration of the unidirectional radiation of the array as a consequence of unequal radiation loads on the two planes. The model also indicates a limited improvement in the unidirectional radiation due to the addition of tuning capacitors in series with the individual projectors.

Security Classification

14. KEY WORDS	LINK A		LINK B		LINK C	
	ROLE	WT	ROLE	WT	ROLE	WT
Acoustic projectors						
Unidirectional radiation						
Multiplanar array						
Biplanar array						
36-element array						
XEM-4B transducer						
Mathematical model						
Transmitting responses						
Back-to-front suppression						

INSTRUCTIONS

1. ORIGINATING ACTIVITY: Enter the name and address of the contractor, subcontractor, grantee, Department of Defense activity or other organization *(corporate author)* issuing the report.

2*a*. REPORT SECURITY CLASSIFICATION: Enter the overall security classification of the report. Indicate whether "Restricted Data" is included. Marking is to be in accordance with appropriate security regulations.

2*b*. GROUP: Automatic downgrading is specified in DoD Directive 5200.10 and Armed Forces Industrial Manual. Enter the group number. Also, when applicable, show that optional markings have been used for Group 3 and Group 4 as authorized.

3. REPORT TITLE: Enter the complete report title in all capital letters. Titles in all cases should be unclassified. If a meaningful title cannot be selected without classification, show title classification in all capitals in parenthesis immediately following the title.

4. DESCRIPTIVE NOTES: If appropriate, enter the type of report, e.g., interim, progress, summary, annual, or final. Give the inclusive dates when a specific reporting period is covered.

5. AUTHOR(S): Enter the name(s) of author(s) as shown on or in the report. Enter last name, first name, middle initial. If military, show rank and branch of service. The name of the principal author is an absolute minimum requirement.

6. REPORT DATE: Enter the date of the report as day, month, year; or month, year. If more than one date appears on the report, use date of publication.

7*a*. TOTAL NUMBER OF PAGES: The total page count should follow normal pagination procedures, i.e., enter the number of pages containing information.

7*b*. NUMBER OF REFERENCES: Enter the total number of references cited in the report.

8*a*. CONTRACT OR GRANT NUMBER: If appropriate, enter the applicable number of the contract or grant under which the report was written.

8*b*, 8*c*, & 8*d*. PROJECT NUMBER: Enter the appropriate military department identification, such as project number, subproject number, system numbers, task number, etc.

9*a*. ORIGINATOR'S REPORT NUMBER(S): Enter the official report number by which the document will be identified and controlled by the originating activity. This number must be unique to this report.

9*b*. OTHER REPORT NUMBER(S): If the report has been assigned any other report numbers *(either by the originator or by the sponsor)*, also enter this number(s).

10. AVAILABILITY/LIMITATION NOTICES: Enter any limitations on further dissemination of the report, other than those imposed by security classification, using standard statements such as:

(1) "Qualified requesters may obtain copies of this report from DDC."

(2) "Foreign announcement and dissemination of this report by DDC is not authorized."

(3) "U. S. Government agencies may obtain copies of this report directly from DDC. Other qualified DDC users shall request through ________________."

(4) "U. S. military agencies may obtain copies of this report directly from DDC. Other qualified users shall request through ________________."

(5) "All distribution of this report is controlled. Qualified DDC users shall request through ________________."

If the report has been furnished to the Office of Technical Services, Department of Commerce, for sale to the public, indicate this fact and enter the price, if known.

11. SUPPLEMENTARY NOTES: Use for additional explanatory notes.

12. SPONSORING MILITARY ACTIVITY: Enter the name of the departmental project office or laboratory sponsoring *(paying for)* the research and development. Include address.

13. ABSTRACT: Enter an abstract giving a brief and factual summary of the document indicative of the report, even though it may also appear elsewhere in the body of the technical report. If additional space is required, a continuation sheet shall be attached.

It is highly desirable that the abstract of classified reports be unclassified. Each paragraph of the abstract shall end with an indication of the military security classification of the information in the paragraph, represented as *(TS)*, *(S)*, *(C)*, or *(U)*.

There is no limitation on the length of the abstract. However, the suggested length is from 150 to 225 words.

14. KEY WORDS: Key words are technically meaningful terms or short phrases that characterize a report and may be used as index entries for cataloging the report. Key words must be selected so that no security classification is required. Identifiers, such as equipment model designation, trade name, military project code name, geographic location, may be used as key words but will be followed by an indication of technical context. The assignment of links, roles, and weights is optional.

Security Classification